Received April 10, 2021, accepted May 5, 2021, date of publication May 10, 2021, date of current version May 18, 2021.

Digital Object Identifier 10.1109/ACCESS.2021.3078608

Analysis of Fractional Order Sliding Mode Control in a D-STATCOM Integrated Power Distribution System

TOQEER AHMED[1,2], ASAD WAQAR[1], RAJVIKRAM MADURAI ELAVARASAN[3], JUNAID IMTIAZ[1], MANOHARAN PREMKUMAR[4], (Member, IEEE), AND UMASHANKAR SUBRAMANIAM[5], (Senior Member, IEEE)

[1]Department of Electrical Engineering, Bahria University, Islamabad 44000, Pakistan
[2]Center for Advanced Electronics and Photovoltaic Engineering (CAEPE), International Islamic University, Islamabad 44000, Pakistan
[3]Clean and Resilient Energy Systems (CARES) Laboratory, Texas A&M University, Galveston, TX 77553, USA
[4]Department of Electrical and Electronics Engineering, Dayananda Sagar College of Engineering, Bengaluru 560078, India
[5]Renewable Energy Laboratory, Department of Communications and Networks, Prince Sultan University, Riyadh 11586, Saudi Arabia

Corresponding authors: Rajvikram Madurai Elavarasan (rajvikram787@gmail.com) and Umashankar Subramaniam (usubramaniam@psu.edu.sa)

ABSTRACT At present, the disturbances like the voltage fluctuations, resulting from the grid's complexities and unbalanced load conditions, create severe power quality concerns like total harmonic distortion (THD) and voltage unbalance factor (VUF) of the grid voltage. Though the custom power devices such as distribution-static compensators (D-STATCOMs) improve these power quality concerns, however, the accompanying controller plays the substantial role. Therefore, this paper proposes a fractional-order sliding mode control (FOSMC) for a D-STATCOM to compensate the low power distribution system by injecting/absorbing a specific extent of the reactive power under disturbances. FOSMC is a non-linear robust control in which the sliding surface is designed by using the Riemann-Liouville (*RL*) function and the chattering phenomenon is minimized by using the exponential reaching law. The stability of FOSMC is evidenced by employing the Lyapunov stability criteria. Moreover, the performance of the proposed FOSMC is further accessed while doing its parametric variations. The complete system is demonstrated with a model of 400V, 180kVA radial distributor along with D-STATCOM under two test scenarios in MATLAB/Simulink environment. The results of the proposed controller are compared with the fixed frequency sliding mode control (FFSMC) and conventional proportional-integral (PI) control. The results validate the superiority of the proposed controller in terms of rapid tracking, fast convergence, and overall damping with very low THD and VUF.

INDEX TERMS Power quality, custom power devices, distribution static compensator, fractional order sliding mode control, total harmonic distortion, voltage unbalance factor.

NOMENCLATURE

Abbreviations:

AMF	Asymmetric Membership Function
CFNN	Compensatory Fuzzy Neural Network
CHBMC	Cascaded H-bridge Multilevel Converter
CSC	Current Source Converter
DC	Direct Current
DCVSA	Discrete Continuous Vortex Search Algorithm
D-STATCOM	Distribution Static Compensator
DG	Distribution Generation
DPC	Direct Power Control
FCS	Finite Control Set
FLC	Fuzzy Logic Control
GOA	Grasshopper's Optimization Algorithm
HV	High Voltage
IP	Integral Proportional
LADRC	Linear Active Disturbance Rejection Control

The associate editor coordinating the review of this manuscript and approving it for publication was Hiu Yung Wong.

LV	Low voltage
MC	Matrix Converter
MG	Microgrid
MPC	Model Predictive Control
NFC	Neuro Fuzzy Control
PID	Proportional Integral Derivative
PLL	Phase Lock Loop
PR	Proportional Resonant
PSO	Particle Swarm Optimization
PV	Photovoltaic
RL	Riemann Liouville
SMC	Sliding Mode Control
SDBC-MMC	Single Delta Bridge Cell-Modular Multi-level cascade converter
SRLMMN	Sign Regressor Least Mean Mixed Norm
SVC	Static VAR Compensator
SPWM	Sinusoidal Pulse Width Modulation
THD	Total Harmonic Distortion
TSA	Tree Seed Algorithm
VSC	Voltage Source Converter
VUF	Voltage Unbalance Factor

I. INTRODUCTION

In the power distribution system, power quality implies to keep the AC bus sinusoidal voltage waveform at the measured voltage and frequency [1]. The waveforms of voltage and current must be purely sinusoidal and free from any interruptions [2]. However, the grid transients and unbalanced loads may distort the waveform and cause voltage instability [3]. These distortions may disseminate all over the power distribution system [4]. Power quality concerns incorporate grid transients (voltage sag/swell), voltage and current distortion, voltage spike, voltage unbalance, noise, harmonics, and flickers. These can initiate abnormal operation of the equipment or assuredly trip the protection devices [5]. To cope with these concerns, fixed and switch reactors/capacitors banks and static VAR compensators (SVC) are established and executed [6]. However, these kinds of standard facilities have a few drawbacks such as large size, additional losses, inadequate bandwidth, and slow response time [7]. The two-level converters can also be employed to compensate the low power distribution system. However, the limited power rating and switching losses of the two-level converters resulting from high-frequency operation in the high power and high voltage applications are considered constraints [8]. In recent times, D-STATCOM has gained enough popularity with the development of semiconductor devices due to its high-power density, small size, minimal losses, fast response, and broad compensation range [9]. D-STATCOM is a power quality conditioner, and capable of supplying and absorbing reactive power, and is integrated into the grid via a VSC as well [10]. D-STATCOM is linked in parallel with the load and can operate uninterruptedly, attaining a power factor near the unity and preventing operational concerns [11]. For reactive power compensation, the D-STATCOM is one of the fastest and most reliable device. By monitoring the magnitude of voltage, the exchange of reactive power between the power distribution system and D-STATCOM can be controlled to alleviate the power quality concerns [12]. Furthermore, an efficient control scheme is also required to rapidly achieve the necessary compensation in a low power distribution system [13].

In recent years, many scholars have accomplished a lot of research work regarding D-STATCOM integration in the power distribution system using linear control strategies. The work in [14], has analyzed the execution of D-STATCOM to reduce the undesirable effect generated by the DG linked to a grid. The voltage profile is improved via the DPC approach employing PI control during steady-state and voltage sag conditions. In [15], the authors have proposed a D-STATCOM to compensate the unbalanced conditions resulting in dc voltage oscillation via PR control. A PID control is employed for SDBC-MMC to compensate the single-phase load in a power distribution system for power factor correction [16]. The authors in [17], have presented a cascaded multi-level inverter-based D-STATCOM during grid transients and load alterations via PI control for reactive power compensation. In [18], the authors have proposed a three-phase four-wire VSC based D-STATCOM using PI control. The D-STATCOM model is utilized under an unbalanced load condition to stabilize the voltage. In [19], the authors have proposed a D-STATCOM for the distribution system to mitigate voltage unbalanced effect created by U-V or V-V winding of transformer employing PI control. In [20], the authors have proposed a D-STATCOM for a renewable energy-based distribution system. The PI control is applied to alleviate the voltage sag/swell problem. The authors in [21], have proposed a CSC-based D-STATCOM which utilizes the minimum DC voltage for the reactive power compensation to eliminate the harmonics and reduces the switching losses using the PI control. In [22], the authors have proposed a combined PV-STATCOM via IP and PID control under an unbalanced non-linear load to reduce the harmonics, zero-sequence component, and the THD. The dynamic response of MG is enhanced by using the D-STATCOM with an improved PID control based on the application of GOA [23]. In [24], the authors have proposed a D-STATCOM based on CSC to enhance the power quality and consistency during step alter in load utilizing PI control. The CHBMC based D-STATCOM using PI control is proposed in [25] to enrich the DC voltage and reactive power control. The control parameters of the PI control are optimized by using the PSO. The authors in [26], have proposed a D-STATCOM to enhance the power quality problem resulted from an unbalanced load condition using the PI control. In [27], the authors have proposed a PI control for parallel operation among D-STATCOMs for the reactive power-sharing, and to compensate the harmonics resulting from the non-linear load. The authors in [28], have proposed a PI control by utilizing the PLL algorithm for a D-STATCOM to enhance the power factor and dc voltage regulation. In [29], the authors have proposed a multi-level CHB D-STATCOM

via PI control to enhance the power factor by eliminating the harmonics and the switching losses. In [30], the authors have investigated the execution of D-STATCOM for reactive power compensation required by doubly-fed wind farm linked to the grid. The power quality concerns alleviated by D-STATCOM in [31] employing PR control and comb filter during unbalanced and non-linear scenarios. Though, the linear control strategies have major limitations such as tuning of control constraints, inadequate transient response [32], and deficient reference tracking in the situation of challenging a significant error [33].

In the context of non-linear control strategies, the authors in [34] have investigated the performance of D-STATCOM via dead-beat repetitive control to diminish the current prediction error for improved reactive power compensation. However, the control has few drawbacks such as parameter variance and external disturbances [35]. The authors in [36] have proposed a D-STATCOM to compensate the unbalanced voltage condition via hysteresis current controller. Though, in the digital platform, the modeling and implementation of hysteresis control are complex and suffer from the variable switching frequency [37]. A PI control based on fuzzy logic is executed for the D-STATCOM to maintain the voltage stability in the power distribution system [38]. Even though, FLC has its limitations due to the fact that it cannot handle situations outside its proposed fuzzy rules, and it is difficult to prove the stability of FLC [39]. The authors in [40], have proposed an NFC for a D-STATCOM during load variations. In [41], the authors have proposed a D-STATCOM via CFNN-AMF controller for the dc voltage regulation and power quality enrichment. However, the dynamic response of the controller is moderate. In [42], a shunt connected D-STATCOM is investigated in the power distribution system to compensate the reactive power required for load balancing. They proposed an SRLMMN control for fast convergence and to reduce steady-state error. The authors in [43], have proposed a cluster balancing control to alleviate the effect of voltage sag from a single-phase, two-phase, and three-phase power distribution system. Despite that, while acknowledging the learning algorithm, the controller needed additional computational time [44]. In [45], the authors have proposed an enhanced LADRC for D-STATCOM to competently control the DC voltage and the reference reactive power during voltage sag and load variations. The authors in [46], have proposed a capacitor-less D-STATCOM based on MC by employing FCS-MPC for reactive power compensation under non-linear load conditions. Though, the switching losses reduce the system reliability due to high fidelity [47]. Thus, an adaptive MPC-based capacitor less D-STATCOM is proposed in [48] to diminish the switching frequency and THD. However, to reach the desired accomplishment the MPC necessitates precise control parameters. Moreover, the cost function calculation requires more computation burden [49]. In [50], the authors have proposed a digital current control for D-STATCOM during unbalanced and non-linear load conditions. The authors in [51], have investigated the execution of D-STATCOM in a T-type configuration by utilizing a simple carrier-based modulation control method to minimize the voltage fluctuation and harmonics at dc link. The optimum location and sizing of D-STATCOM are determined in [52] by employing DCVSA to reduce the operational cost. In [53], the authors have proposed a novel TSA-based D-STATCOM to improve the execution and consistency during normal and critical load conditions.

Sliding mode control is a well-known non-linear control that offers robustness, fast dynamic response, stability, enhanced regulation properties, and highly compatible with power converters [54]. An SMC is employed for a D-STATCOM evaluation and design [55] to compensate the power distribution system under voltage sag. Nevertheless, the control eliminates the chattering problem and stabilizes the output voltage to some extent. Despite this, the response time is very slow which may cause stability issues. The authors in [56], have proposed a three-level four-leg D-STATCOM for reactive power compensation using second-order SMC during grid faults and unbalanced load circumstances. Though, mathematical modeling and execution are quite complex. Moreover, during unbalanced load conditions, the THD of the output is high as well. The authors in [57], have proposed and investigate the performance of a D-SATCOM based on wind farm DFIG via fractional-order SMC. Nevertheless, the voltage unbalance factor (VUF) is not taken into account under unbalanced load conditions. In [58], a photovoltaic (PV) based D-STATCOM is investigated under harmonics and load variations while utilizing SMC. Though, the robustness and tracking error of this control scheme is nearly degraded. An integral SMC is employed for a D-STATCOM to compensate the load alterations [59]. Although, the control provides a good tracking response under unbalanced load conditions. Nevertheless, the output voltage waveform indicates the chattering problem and stability issue as well. In [60], the authors have proposed an SMC for a cascaded STATCOM to compensate the voltage unbalance and voltage sag problem. Although, the response time of control to reach a steady-state is very slow. In [61], the authors have investigated the performance of D-STATCOM by using the input-output feedback linearization scheme. They have proposed SMC to improve the three-phase voltage at LV AC bus and dc side voltage of D-STATCOM. Though, the robustness of the controller is lacking. In [62], the authors have proposed an SMC for D-STATCOM under DC link voltage variations to enrich the system stability. The authors in [63], have proposed an SMC for the D-STATCOM to eliminate the harmonics created by nonlinear load. Nevertheless, the size and cost of the system is increase due to large values of output filter selected to eliminate the harmonics. The authors in [64] have proposed an enhanced D-STATCOM model under voltage sag/swell using SMC. The authors claim that the system efficiency increases, although its performance is inadequate in terms of THD under voltage sag/swell.

After a comprehensive review of the literature survey, following conclusions could be drawn.

- The key emphasis of the D-STATCOM based power distribution system is to improve the power quality in the low power distribution systems.
- As a result of the escalating number of power electronic devices, grid transients, and sensitive loads, the future trend highly demands improved power quality in the low power distribution systems by employing the D-STATCOM. Consequently, more advanced controller is required to tackle these problems. The application of a non-linear robust controllers is found deficient in the published literature.
- The FOSMC is not implemented in the literature studies for power quality problems such as grid transients (voltage sag/swell) and unbalanced load conditions.
- Besides, the performance of the FOSMC under its parametric variations on a D-STATCOM is found missing.
- The stability analysis of the applied controllers, and the phenomenon of chattering elimination is deficient as well.
- The essential measure VUF for evaluating a controller under unbalanced load conditions has been seen to be lacking in published literature for this particular problem.

In this paper, the authors have proposed the FOSMC for D-STATCOM to compensate the low power distribution system under disturbances. A model of radial distributor along with D-STATCOM is examined under grid transients (voltage sag/swell) and unbalanced load conditions. The D-STATCOM injects/absorbs the specific amount of reactive power at the LV AC bus depending upon the disturbances. Besides, the performance of the FOSMC under its parametric variations on a D-STATCOM is discussed as well. In the aspect of robustness, the FOSMC is superior by virtue of its additional design parameters comprising of adjustable non-integer differentiator and integrator [65]. This improves the dynamic response of the system, establishes more degree of freedom, ensures the fast convergence, and gives an adequate method to eliminate the chattering phenomenon [66]. The conventional SMC has certain challenges such as chattering phenomenon and inadequate convergence which might result in unpredicted high-frequency oscillations and diminish the system execution [67]. FOSMC strategy, even though confirms to be competent of alleviating the chattering intensity in the sliding surface and quickening the reaching speed as well [68]. In this paper, the Riemann-Liouville (*RL*) function is utilized to design the sliding surface. Furthermore, the stability of the FOSMC is evidenced by employing Lyapunov stability criteria. To summarize, the authors' key contributions include:

- The D-STATCOM integrated power system is proposed to improve the power quality under disturbances.
- Two test scenarios have been established and examined. The grid transients (voltage sag/swell) are considered at the LV AC bus in the first scenario. Likewise, in second scenario an unbalanced load conditions are considered at the LV AC bus. D-STATCOM sustains the voltage at LV AC bus by injecting/absorbing a certain extent of reactive power in both cases.
- FOSMC is proposed to drive the D-STATCOM under the disturbances.
- Besides, performance of the FOSMC under its parametric variations on a D-STATCOM is discussed as well.
- The sliding surface of the proposed FOSMC is designed by using the Riemann Liouville (*RL*) function. Additionally, the chattering phenomenon is minimized by using the exponential reaching law.
- The stability of the FOSMC is evidenced by employing Lyapunov stability criteria.
- The THD and VUF of the output voltage have been considered to evaluate the controller's performance.
- Furthermore, the experimental results of the proposed control are compared with FFSMC and PI control as well.
- The performance of proposed FOSMC outperformed the literature study reference [57] in terms of controller robustness and limited scope of study.

Rest of the paper is arranged in the following approach. Section II describes the model structure, design, and control of D-STATCOM. Section III derives the mathematical modelling of FOSMC for D-STATCOM. Section IV proves the stability of proposed FOSMC. Section V made the results and discussions. Section VI concludes the paper.

II. MODEL STRUCTURE, DESIGN, AND CONTROL OF D-STATCOM

Fig. 1 shows the simplified model of D-STATCOM configuration [69] which includes a Y-Δ and Δ-Δ distribution transformer, dynamic load (linear and unbalanced), main grid, and a D-STATCOM.

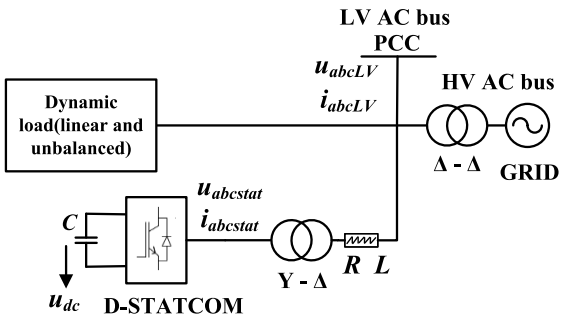

FIGURE 1. Simplified model of D-STATCOM configuration.

The main grid is linked at the LV AC bus via Δ-Δ distribution transformer. The 1500V D-STATCOM [70] is linked in shunt with the main grid via Y-Δ distribution transformer at LV AC bus and connected to a capacitor by its dc bus. The magnitude of the voltage generated by a D-STATCOM is not the same as grid voltage, although have the same phase. The compensation process of the D-STATCOM is altered on the

divergence among voltage at LV AC bus and D-STATCOM voltage. A D-STATCOM injects the reactive power while considered $u_{abcstat}$ is higher than u_{abcLV}. Likewise, a D-STATCOM absorbs the reactive power while considered $u_{abcstat}$ is lower than u_{abcLV}. To design the three-phase D-STATCOM, the value of C_{dc} can be obtained by using Eq. (1) [70]

$$C_{dc} = \frac{3u_s \Delta I_L T}{u_{c\max}^2 - u_{dc}^2} \tag{1}$$

where, C_{dc}, u_{dc}, u_{cmax}, $\Delta I_{\rm L}$, $u_{\rm s}$, and T denotes the dc capacitor, capacitor voltage, pre-set threshold of capacitor voltage, 5% of load current (current ripple ratio), D-STATCOM peak phase voltage, and time period of one cycle, respectively. The high harmonics that are multiples of switching frequency are removed by using the three-phase filter. In the absence of a filter, the noise will add in line with injected voltages. To overcome this problem, an LC filter is utilized at the secondary side of the distribution transformer. The value of the filter inductor and capacitor is chosen appropriately by using Eq. (2) [87] and Eq. (3) [88].

$$L = \frac{\sqrt{3} m u_{dc}}{12 f_s a \Delta I_L} \tag{2}$$

$$f_s = \frac{1}{2\pi\sqrt{LC}} \tag{3}$$

where, terms m, f_s, a indicates modulation index, switching frequency, and overloading factor, respectively. Fig. 2 shows the proposed D-STATCOM control scheme. The three-phase voltages and currents (u_{abcLV}, i_{abcLV}, $u_{abcstat}$, $i_{abcstat}$) are signified as the voltages and currents at LV AC bus and D-STATCOM output. While the transformer and line parameters are characterized by R and L. The direct quadrature (dq) approach is applied to both voltages and currents to enhanced reference tracking for FOSMC loops and respective SPWM gate signal generation. The transformation angle θ is sensed at the LV AC bus by applying a PLL. Fig. 3 represents the flowchart of the D-STATCOM compensation procedure.

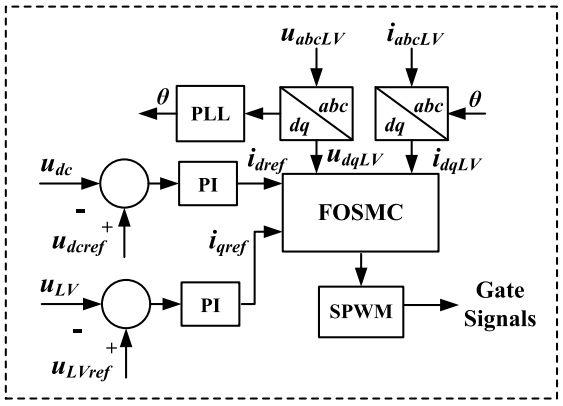

FIGURE 2. Proposed D-STATCOM control scheme.

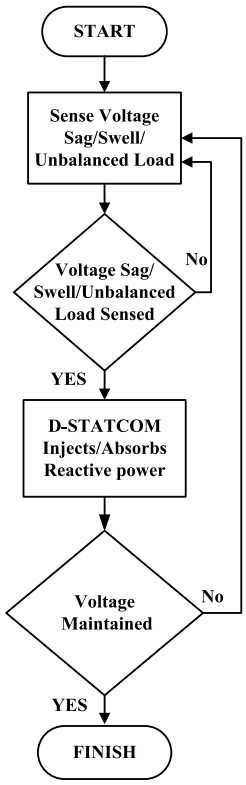

FIGURE 3. Flowchart of D-STATCOM compensation procedure.

III. MATHEMATICAL MODEL OF D-STATCOM USING FRACTIONAL ORDER SLIDING MDOE CONTROL

The D-STATCOM dynamics in *abc*-stationary reference frame is modelled as [72]

$$\frac{di_{abcLV}}{dx} = \frac{-Ri_{abcLV}}{L} + \frac{u_{abcstat}}{L} - \frac{u_{abcLV}}{L} \tag{4}$$

In synchronous reference frame (dq structure) along with addition of D-STATCOM modulating signal ($u_{stat} = u_{dc}/2)m$, and $\omega = d\theta/dt$, Eq. (4) can be modified as

$$\frac{di_{dLV}}{dt} = \frac{-Ri_{dLV}}{L} + \omega i_{qLV} + \frac{u_{dc}m}{2L} - \frac{u_{dLV}}{L} \tag{5}$$

$$\frac{di_{qLV}}{dt} = \frac{-Ri_{qLV}}{L} - \omega i_{dLV} + \frac{u_{dc}m}{2L} - \frac{u_{qLV}}{L} \tag{6}$$

With the addition of model uncertainty terms (ρ_d, ρ_q) [65], Eq. (5) and Eq. (6) can be modified as

$$\frac{di_{dLV}}{dt} = f_d(u_{dLV}, u_{qLV}, i_{dLV}, i_{qLV}) + xm_d + \rho_d \tag{7}$$

$$\frac{di_{qLV}}{dt} = f_q(u_{dLV}, u_{qLV}, i_{dLV}, i_{qLV}) + xm_q + \rho_q \tag{8}$$

where,

$$x = \frac{u_{dc}}{2L} \tag{9}$$

The most significant cause of model uncertainties includes variation in system parameters such as mechanical stresses,

expansion, self-thermal alterations, load demand, a failure rate of transmission lines, generation output, line outage and generator outage [83] can significantly disrupt the system stability and reduces the system performance [84]. The influence of uncertain parameters is usually not substantial for unstressed systems. When the stability margin declines, though, system behavior becomes considerably additional sensitive to parameter perturbations [85]. In this aspect, the robust FOSMC is designed against external disturbance and parameter uncertainties. Besides, the utilization of fractional-order differentiator and integrator offers an extra degree of freedom and enhances the system convergent properties [86].

The non-linear functions terms $f_d(.)$ and $f_q(.)$ are described as

$$f_d = \frac{di_{dLV}}{dt} = \frac{-Ri_{dLV}}{L} + \omega i_{qLV} - \frac{u_{dLV}}{L} \tag{10}$$

$$f_q = \frac{di_{qLV}}{dt} = \frac{-Ri_{qLV}}{L} - \omega i_{dLV} - \frac{u_{qLV}}{L} \tag{11}$$

The proposed FOSMC non-integer sliding surface for d and q control loops are described as [69]

$$S_d = e_d + \lambda D^{\alpha-1}(sig(e_d)^{\gamma}) \tag{12}$$

$$S_q = e_q + \lambda D^{\alpha-1}(sig(e_q)^{\gamma}) \tag{13}$$

where,

$$e_d = i_{dref} - i_{dLV} \tag{14}$$

$$e_q = i_{qref} - i_{qLV} \tag{15}$$

The e_d and e_q terms are related to signify current reference tracking error, $D^{\alpha-1}$ signifies the fractional integral term of $(\alpha - 1)$ order, and α, γ, λ signifies the positive parameters along design choices of ($\alpha < 1$ and $\gamma < 1$).

The well-known $sig(.)^{\gamma}$ function is described as [65]

$$sig(x)^{\gamma} = |x|^{\gamma}\, sgn(x) \tag{16}$$

where, $sgn(.)$ signifies the sign function described as

$$sgn(x) = \begin{cases} \dfrac{x}{|x|}, & if\ x \neq 0 \\ 0, & if\ x = 0 \end{cases} \tag{17}$$

Now taking the derivative of Eq. (12) and Eq. (13) and substituting the Eq. (14) and Eq. (15) into Eq. (12) and Eq. (13), the proposed sliding surface equation with the inclusion of RL function [73] is written as

$$S_d^{\bullet} = i_{dref}^{\bullet} - i_{dLV}^{\bullet} + \lambda_{RL} D^{\alpha}(sig(e_d)^{\gamma}) \tag{18}$$

$$S_q^{\bullet} = i_{qref}^{\bullet} - i_{qLV}^{\bullet} + \lambda_{RL} D^{\alpha}(sig(e_q)^{\gamma}) \tag{19}$$

By substituting Eq. (10) and Eq. (11) into Eq. (18) and Eq. (19), the modified equation can be written as

$$S_d^{\bullet} = f_d(.) + xm_d + \rho_d + \lambda_{RL} D^{\alpha}(sig(e_d)^{\gamma}) \tag{20}$$

$$S_q^{\bullet} = f_q(.) + xm_q + \rho_q + \lambda_{RL} D^{\alpha}(sig(e_q)^{\gamma}) \tag{21}$$

Based on Eq. (20) and Eq. (21), the proposed control law ensures the current reference tracking error convergence and generate the modulating signals m_d and m_q for SPWM can be written as

$$m_d = \frac{-[f_d(.) + \lambda_{RL} D^{\alpha}(sig(e_d)^{\gamma}) + k_d sgn(s_d)]}{x} \tag{22}$$

$$m_q = \frac{-[f_q(.) + \lambda_{RL} D^{\alpha}(sig(e_q)^{\gamma}) + k_q sgn(s_q)]}{x} \tag{23}$$

where, terms k_d and k_q signifies the FOSMC sliding gains. Fig. 4 shows the control diagram of FOSMC for D-STATCOM in q-axis. Likewise, same methodology is adopter for d-axis. Fg. 5 shows the flowchart of proposed FOSMC strategy.

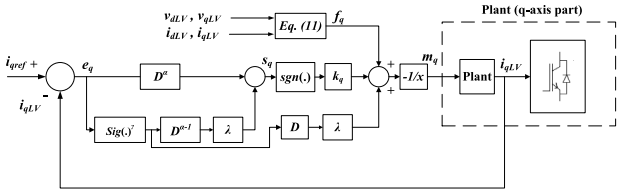

FIGURE 4. Control diagram of FOSMC for D-STATCOM in q-axis.

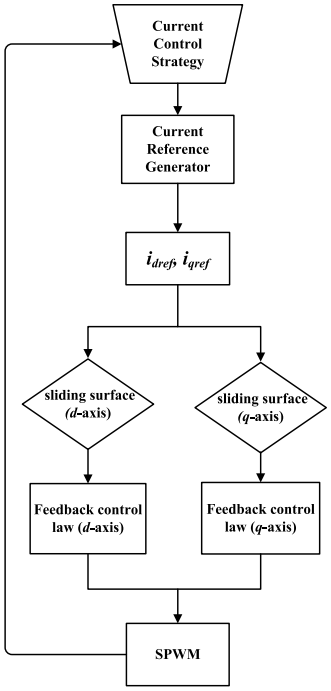

FIGURE 5. Flowchart of FOSMC strategy.

IV. STABILITY ANALYSIS

Considering the definition of Lyapunov function for the stability of proposed FOSMC is described as [74]

$$V(t) = \frac{1}{2}(S_d^2 + S_q^2) \tag{24}$$

By taking the time derivative of Eq. (24) one obtains

$$V^{\bullet}(t) = S_d S_d^{\bullet} + S_q S_q^{\bullet} \tag{25}$$

Based on Eq. (7) and Eq. (8), and Eq. (25) the time derivative Lyapunov function signified as

$$V^{\bullet}(t) = S_d(f_d(.) + xm_d + \rho_d + \lambda_{RL}D^{\alpha}(sig(e_d)^{\gamma}) + S_q(f_q(.) + xm_q + \rho_q + \lambda_{RL}D^{\alpha}(sig(e_q)^{\gamma}) \quad (26)$$

By substituting m_d and m_q from Eq. (22) and Eq. (23) into Eq. (26), the modified equation is written as

$$V^{\bullet}(t) = S_d(\rho_d - k_d sgn(S_d)) + S_q(\rho_q - k_q sgn(S_q)) \quad (27)$$

Considering $sgn(S_d) = |S_d|/S_d$ and $sgn(S_q) = |S_q|/S_q$

$$V^{\bullet}(t) = (S_d\rho_d - k_d|S_d|) + (S_q\rho_q - k_q|S_q|) \quad (28)$$

Now selecting $(k_d = |\rho_d| + \xi_d)$ and $(k_q = |\rho_q| + \xi_q)$, where ξ_d and ξ_q signify as positive parameters. Eq. (28) one finds

$$V^{\bullet}(t) \leq -\xi_d|S_d| - \xi_q|S_q| \leq -\min(\xi_d.\xi_q)(|S_d| + |S_q|) = -\min(\xi_d.\xi_q)\|S\|_1 \quad (29)$$

The minimum value of ξ_d and ξ_q represents minimum (ξ_d, ξ_q). Eq. (29) verifies the stability condition and finite time convergence of proposed FOSMC sliding surface S_d and S_q. Consequently, $V^{\cdot}(t)$ is negative, and the proposed FOSMC system is asymptotic stable [69].

Remarks:

Afterwards the reaching condition is guaranteed, the Lemma (Lyapunov stability theorem) can be conferred to examine the system stability during the sliding phase.

Lemma 1: The system is asymptotic stable approaching 0 when the positive definite function $V(t) > 0$ exists and satisfy $V^{\cdot}(t) < 0$, and $V(t)$ is negative definite [81].

Lemma 2: The system is unstable approaching 0 when the positive definite function $V(t) > 0$ exists and satisfy $V^{\cdot}(t) > 0$, and $V(t)$ is positive definite [82].

V. SYSTEM BASED ANALYSIS AND RESULT DISCUSSIONS

In this section, a detailed model of D-STATCOM, based on Fig. 1 [69] has been developed and accomplished in MATLAB Simulink environment to validate the performance of the proposed FOSMC under two test scenarios. Besides, the performance of the FOSMC under its parametric variations on a D-STATCOM is discussed as well. The implementation of the proposed FOSMC is compared with FFSMC and PI control. In the first test scenario, the main grid signified by a power generator resulting in grid transients (voltage sag/swell) at the LV AC bus. In the second test scenario, the voltage and current are unbalanced, resulting from unbalanced load conditions at the LV AC bus. D-STATCOM injects/absorbs the required reactive power to keep the constant voltage at the LV AC bus in both scenarios. The parameters of the proposed power distribution system are presented in TABLE 1 [69]. The control parameters of the proposed FOSMC and FFSMC are presented in TABLE 2 [69] and TABLE 3 [75], respectively. The parameters of PI control are chosen according to the optimal setting to achieve fast output stabilization and are presented in TABLE 4 [76].

TABLE 1. Parameters of proposed electrical power distribution system.

Symbol	Parameter	Value
u_{LV}	Nominal Voltage at LV AC bus	312V
L_{ac}	Dynamic Load	50kVA
ω	Angular Frequency	3.77rad/s
L	Coupling Inductance of D-STATCOM	2.89mH
R	Coupling Resistance D-STATCOM	0.1mH
f_s	Switching Frequency of D-STATCOM	10kHz
Q	Nominal Power of D-STATCOM	±50kVAR
u_{dc}	DC Link Voltage of D-STATCOM	1500V

TABLE 2. Parameters of fractional order SMC.

Symbol	Parameter	Value
γ	Fractional Order SMC Parameter	0.9
λ	Fractional Order SMC Parameter	1500
α	Fractional Order SMC Coefficient	0.5
k_d, k_q	Fractional Order Sliding Gains	$5x10^6$

TABLE 3. Parameters of fixed frequency SMC.

Symbol	Parameter	Value
ε_d	Fixed Frequency SMC Parameter	200
k_d	Fixed Frequency SMC Gain	100
ε_q	Fixed Frequency SMC Parameter	200
k_q	Fixed Frequency SMC Gain	50

TABLE 4. Parameters of PI control.

Symbol	Parameter	Value
k_{pi}	Proportional Gain (Current Loop)	1
k_{ii}	Integral Gain (Current Loop)	3.3
k_{pv}	Proportional Gain (Voltage Loop)	5
k_{iv}	Integral Gain (Voltage Loop)	10

A. STEADY STATE PERFORMANCE AND FOSMC PARAMETERS SELECTION

The proposed FOSMC accomplishment is based on its control parameter variations [77]. Besides, the resemblance between proposed FOSMC, FFSMC, and PI control strategies required a steady-state test to evaluate the execution. The foremost concerns of the execution assessment are the chattering phenomenon and amplitude of the error signal [78]. The chattering phenomenon ruins the system stability and is accounted as a low order noise in the power distribution system [73]. Due to the instability of error signals among error boundaries, the chattering problem is created [77]. The conventional SMC does not have any control on chattering phenomena however the FOSMC is competent to diminish the error signal and convergence within the fraction of chattering time interval via choosing the suitable value of fractional coefficient α [65]. The fractional-order can be selected by examining the complete realization of control outcomes with varied control parameters. The increase of fractional coefficient α reduces the effect of the $(D^{\alpha-1}(sig(e_d)^{\gamma}))$ integral term on the FOSMC sliding surface, and simultaneously increases the signal tracking error [65], and reduces the convergence time [69]. Similarly, due to the presence of model

uncertainties and external disturbances, the fractional order sliding gains k_d and k_q are chosen to satisfy the reaching condition [79].

B. PERFORMANCE EVALUATION UNDER VOLTAGE SAG/SWELL OF MAIN GRID

In this test scenario, the proposed D-STATCOM model employing FOSMC is evaluated under voltage sag/swell in an entire simulation of 0.2s. Initially, the nominal voltage of 312V is maintained at LV AC bus under normal conditions. The voltage sag initiates at 0.05s results in a voltage decline of 10% at LV ac bus. Similarly, voltage swell initiates at 0.1sec results in a voltage rise of 10% at LV AC bus. The system returns to normal condition in the simulation time of 0.15s. Fig. 6(a) shows the three-phase voltage waveform at LV AC bus during voltage sag/swell. Fig. 6(b) shows the RMS voltage waveform at LV AC bus during voltage sag/swell. Fig. 6(c) shows the load active and reactive power waveform under voltage sag/swell.

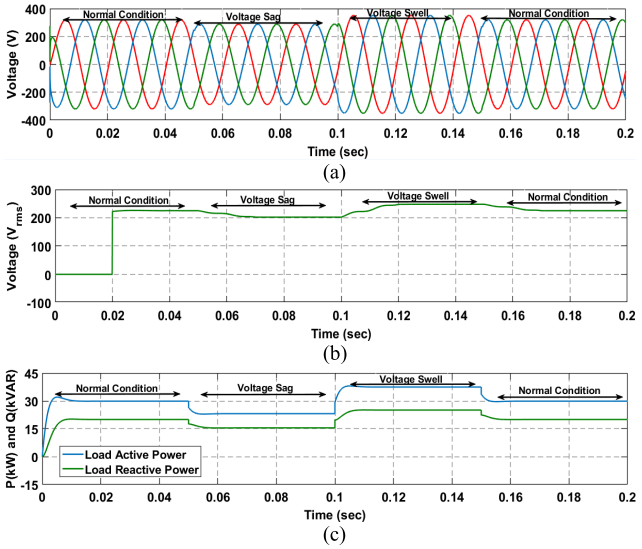

FIGURE 6. (a) Three-phase voltage at LV AC bus under voltage sag/swell of Main Grid (b) RMS Voltage at LV AC bus under voltage sag/swell of Main Grid (c) Load Active and Reactive power under voltage sag/swell of main grid.

Besides the operation of the proposed D-STATCOM, the voltage at the LV AC bus is made constant under voltage sag/swell. The D-STATCOM maintains the voltage at the LV AC bus while injects/absorbs the reactive power required. Fig. 7(a) and Fig. 7(b) shows the three-phase and RMS voltage waveform at LV AC bus during voltage sag/swell with D-STATCOM while employing PI control. Fig. 7(c) and Fig. 7(d) shows the three-phase and RMS voltage waveform at LV AC bus during voltage sag/swell with D-STATCOM while employing FFSMC. Fig. 7(e) and Fig. 7(f) shows the three-phase and RMS voltage waveform at LV AC bus during voltage sag/swell with D-STATCOM while employing FOSMC. Nevertheless, the execution of the proposed FOSMC is extremely exceptional regarding rapid reference

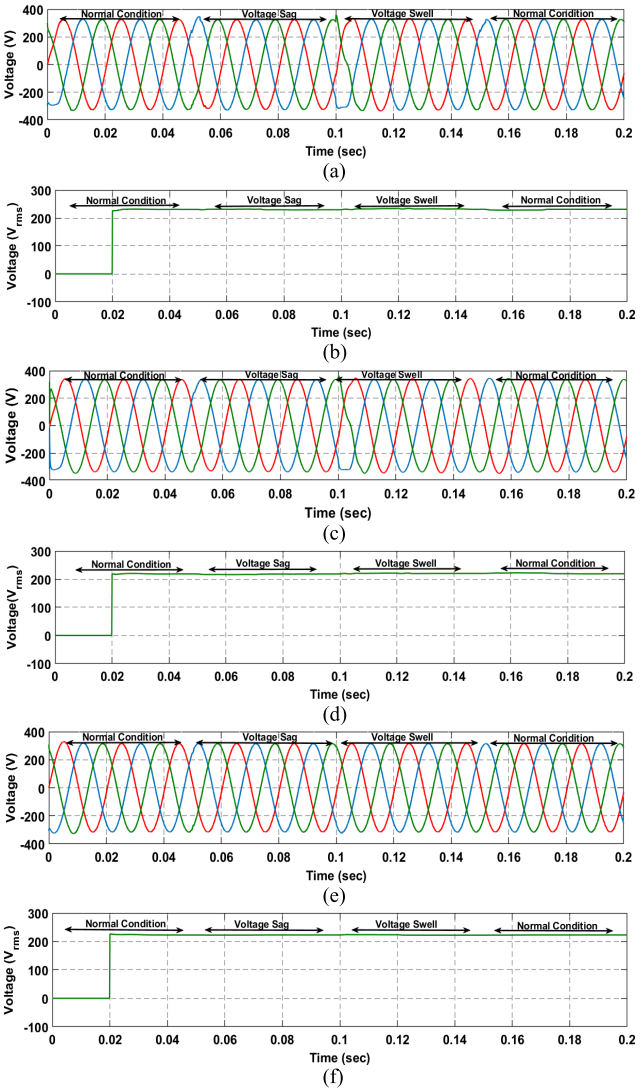

FIGURE 7. (a) Three-phase Voltage at LV AC bus under voltage sag/swell of main Grid with D-STATCOM while employing PI control (b) RMS Voltage at LV AC bus under voltage sag/swell of main Grid with D-STATCOM while employing PI control (c) Three-phase Voltage at LV AC bus under voltage sag/swell of main Grid with D-STATCOM while employing FFSMC (d) RMS Voltage at LV AC bus under voltage sag/swell of main Grid with D-STATCOM while employing FFSMC (e) Three-phase Voltage at LV AC bus under voltage sag/swell of main Grid with D-STATCOM while employing FOSMC (f) RMS Voltage at LV AC bus under voltage sag/swell of main Grid with D-STATCOM while employing FOSMC.

tracking and fast convergence in contrast to FFSMC and PI control. The assessment of voltage THD at LV AC bus during voltage sag/swell is listed in TABLE 5. It is evident that the voltage THD of proposed FOSMC during voltage sag/swell results in 0.52% in contrast to FFSMC and PI control and are well under the IEEE standards which verifies the competency and exceptional performance of proposed control.

Fig. 8(a) shows the load active and reactive power under voltage sag/swell with D-STATCOM at LV AC bus while employing PI control. Similarly, Fig. 8(b) shows the load active and reactive power under voltage sag/swell with D-STATCOM at LV AC bus while employing FFSMC.

TABLE 5. Assessment of voltage THD at LV AC bus during voltage Sag/Swell.

Controller Strategy	Load Type	THD (%)
PI Control	Balanced load	2.17
FFSMC	Balanced load	0.84
FOSMC	Balanced load	0.52

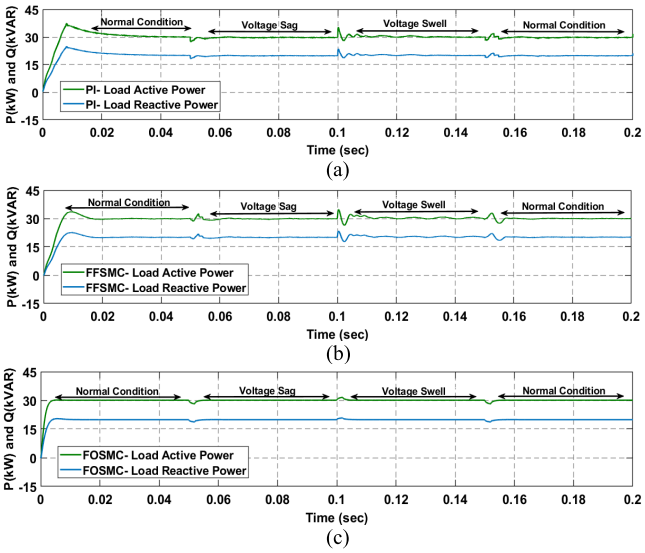

FIGURE 8. (a) Load Active and Reactive power under voltage sag/swell with D-STATCOM while employing PI control (b) Load active and reactive power under voltage sag/swell with D-STATCOM while employing FFSMC (c) Load active and reactive power under voltage sag/swell with D-STATCOM while employing FOSMC.

Fig. 8(c) shows the load active and reactive power under voltage sag/swell with D-STATCOM at LV AC bus while employing FOSMC. The execution of the proposed FOSMC can be seen exceptional in terms of fast convergence, upright damping, and instant tracking, in distinction to PI control and FFSMC.

Fig. 9(a) shows the injected/absorbed reactive power by D-STATCOM under voltage sag/swell while employing PI control. Fig. 9(b) shows the injected/absorbed reactive power by D-STATCOM under voltage sag/swell while employing FFSMC. Fig. 10 shows the variation of α, k_d and k_q, and its influence on rise time, convergence time, tracking error, and time to reach the steady-state under voltage sag/swell. The optimum value of α can be retrieved by varying it from 0 to 0.9. Initially, the value of the fractional coefficient α is chosen from [65]. From Fig. 10(a), it can be observed that the increase of $\alpha = 0.8$ increases the tracking error and chattering. Likewise, the decrease of $\alpha = 0.2$ increases the overshoot, rise time, and time to reach the steady-state, can be seen in Fig. 10(c). In the context of k_d and k_q, the initial values are selected from [69]. The decrease in the values of k_d and k_q results in the increase of tracking error and the time to reach the steady-state and it can be seen in Fig. 10(d). Meanwhile, the increase of k_d and k_q results in the decrease of tracking error and the time to reach the steady-state. Therefore, the value of FOSMC parameters must be selected in such a way that a compromise is achieved among the rise time, overshoot, convergence time, tracking error, and chattering free smooth output. The reference reactive power value is admirable tracked by the controlled trajectories when α is selected to be 0.5, and k_d, k_q are selected to be 5×10^6, evidenced in Fig. 10(b). The peak overshoot and convergence

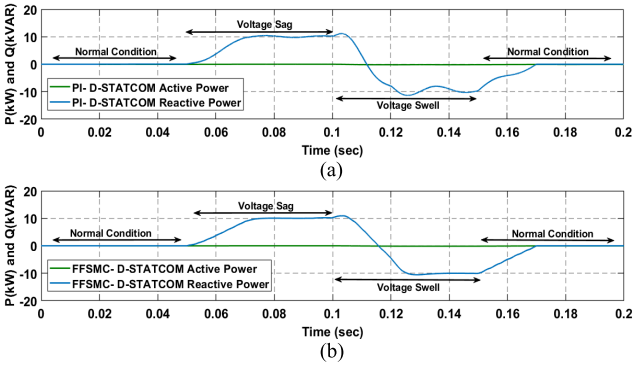

FIGURE 9. (a) Injected/absorbed Reactive power by D-STATCOM under voltage sag/swell while employing PI control (b) Injected/absorbed Reactive power by D-STATCOM under voltage sag/swell while employing FFSMC.

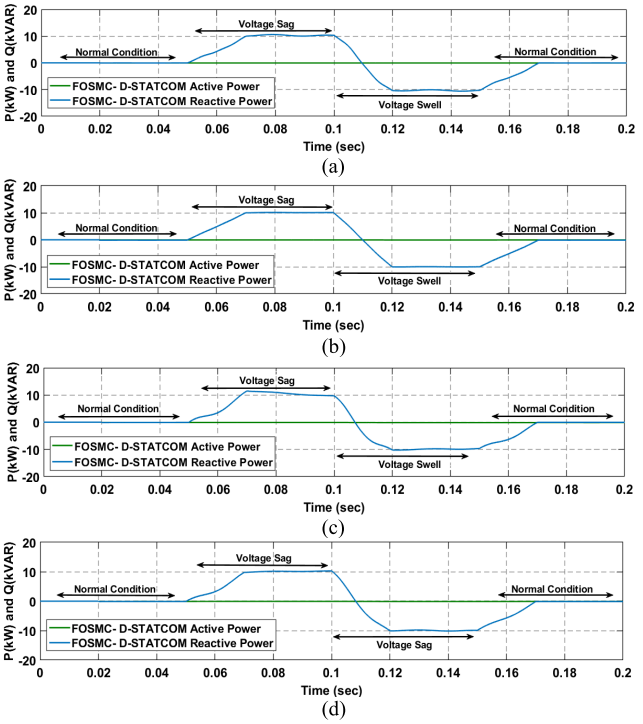

FIGURE 10. (a) Injected/absorbed reactive power by D-STATCOM under voltage sag/swell while employing FOSMC with $\alpha = 0.2$ and k_d, $k_q = 5 \times 10^6$ (b) Injected/absorbed reactive power by D-STATCOM under voltage sag/swell while employing FOSMC with $\alpha = 0.5$ and k_d, $k_q = 5 \times 10^6$ (c) Injected/absorbed reactive power by D-STATCOM under voltage sag/swell while employing FOSMC with $\alpha = 0.8$ and k_d, $k_q = 5 \times 10^6$ (d) Injected/absorbed reactive power by D-STATCOM under voltage sag/swell while employing FOSMC with $\alpha = 0.5$ and k_d, $k_q = 3 \times 10^4$.

time are enhanced because of non-integer order instantaneous error as per the major characteristic of FOSMC. It can be noted that the proposed FOSMC illustrates the exceptional execution over the FFSMC and PI control in the reactive power tracking, due to the fact that the proposed FOSMC is competent of precisely tracking the reference value with the lowest chattering.

Fig. 11(a) shows the dc voltage of D-STATCOM under voltage sag/swell while employing PI control. Fig. 11(b) shows the dc voltage of D-STATCOM under voltage sag/swell while employing FFSMC. Fig. 11(c) shows the dc voltage of D-STATCOM under voltage sag/swell while employing the proposed FOSMC. It can be noted that the execution of the proposed FOSMC is superior to FFSMC and PI control regarding fast convergence and fast-tracking.

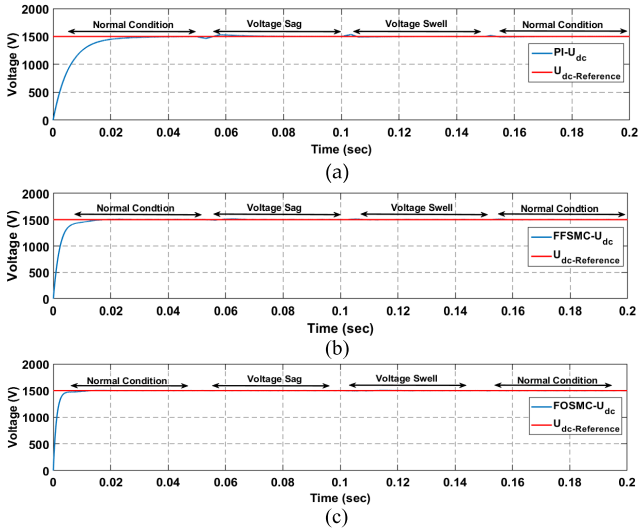

FIGURE 11. (a) dc voltage of D-STATCOM under voltage sag/swell while employing PI Control (b) dc voltage of D-STATCOM under voltage sag/swell while employing FFSMC (c) dc voltage of D-STATCOM under voltage sag/swell while employing FOSMC.

C. PERFORMANCE EVALUATION UNDER UNBALANCED LOAD CONDITIONS

In this test scenario, the proposed D-STATCOM model employing FOSMC is evaluated under unbalanced load conditions in an entire simulation of 0.2s. Initially, the balanced load of $P = 30$ kW and $Q = 20$ kVAR is applied to the system. At 0.07sec, a balanced load is disconnected from the system and an unbalanced load of ($P = 31$ kW and $Q = 18$ kVAR for phase a, $P = 29$ kW and $Q = 17$ kVAR for phase b, $P = 32$ kW and $Q = 22$ kVAR for phase c) is imposed on the system, results in distorted current waveform at LV AC bus, and subsequently, the voltage also got distorted. At 0.15s, the unbalanced load is switch off and a normal load is again imposed on the system. Fig. 12(a) and Fig. 12(b) shows the three-phase and RMS current at the LV AC bus under unbalanced load conditions. Fig. 12(c) and Fig. 12(d) shows the three-phase and RMS distorted voltage at the LV AC bus resulting from an unbalanced current.

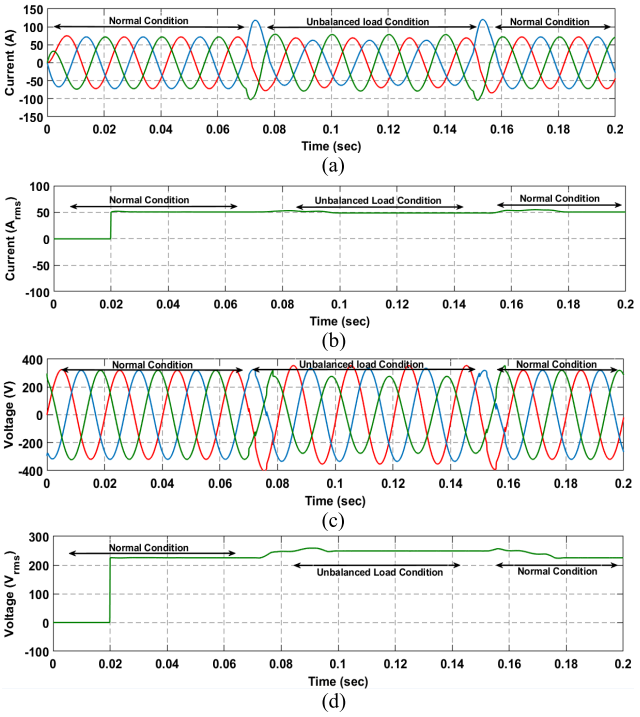

FIGURE 12. (a) Three-phase Current at LV AC bus under unbalanced load condition (b) RMS Current at LV AC bus under unbalanced load condition (c) Three-phase Voltage at LV AC bus under unbalanced load condition (d) RMS Voltage at LV AC bus under unbalanced load condition.

Besides the operation of the proposed D-STATCOM, the voltage at the LV AC bus is made constant under unbalanced load conditions. The D-STATCOM maintains the voltage at the LV AC bus while injecting the reactive power required. Fig. 13(a) and Fig. 13(b) shows the three-phase and RMS voltage at LV AC bus under unbalanced load conditions with D-STATCOM while employing PI control. Fig. 13(c) and Fig. 13(d) shows the three-phase and RMS voltage at LV AC bus under unbalanced load conditions with D-STATCOM while employing FFSMC. Fig. 13(e) and Fig. 13(f) shows the three-phase and RMS voltage at LV AC bus under unbalanced load conditions with D-STATCOM while employing FOSMC. However, the execution of the proposed FOSMC is extremely exceptional regarding rapid reference tracking and fast convergence in contrast to FFSMC and PI control. The assessment of voltage THD and VUF at LV AC bus during unbalanced load conditions is reported in TABLE 6. It can be observed that the voltage THD and VUF of proposed FOSMC during unbalanced load conditions result in 0.97% and 0.0014% in contrast to FFSMC and PI control and are well under the IEEE standards which verifies the competency and exceptional performance of FOSMC.

Fig. 14(a) shows the load active and reactive power under unbalanced load conditions with D-STATCOM at LV AC bus while employing PI control. Similarly, Fig. 14(b) shows the load active and reactive power under unbalanced load conditions with D-STATCOM at LV AC bus while employing FFSMC. Fig. 14(c) shows the load active and reactive power

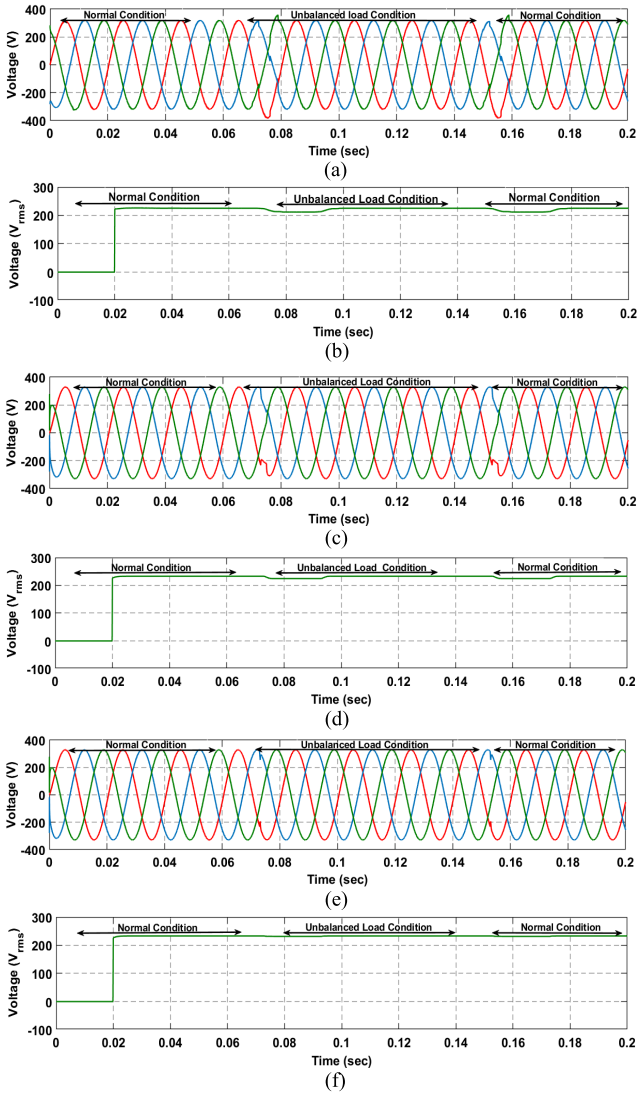

FIGURE 13. (a) Three-phase Voltage at LV AC bus under unbalanced load condition with D-STATCOM while employing PI control (b) RMS Voltage at LV AC bus under unbalanced load condition with D-STATCOM while employing PI control (c) Three-phase Voltage at LV AC bus under unbalanced load condition with D-STATCOM while employing FFSMC (d) RMS Voltage at LV AC bus under unbalanced load condition with D-STATCOM while employing FFSMC (e) Three-phase Voltage at LV AC bus under unbalanced load condition with D-STATCOM while employing FOSMC (f) RMS Voltage at LV AC bus under unbalanced load condition with D-STATCOM while employing FOSMC.

TABLE 6. Assessment of voltage THD at LV AC bus during unbalanced load conditions.

Controller Strategy	THD (%)	VUF (%)
PI Control	3.63	0.71
FFSMC	1.96	0.02
FOSMC	0.97	0.0014

under unbalanced load conditions with D-STATCOM at LV AC bus while employing FOSMC. The execution of the proposed FOSMC can be seen exceptional in terms of fast convergence, upright damping, and instant tracking, in distinction to PI control and FFSMC.

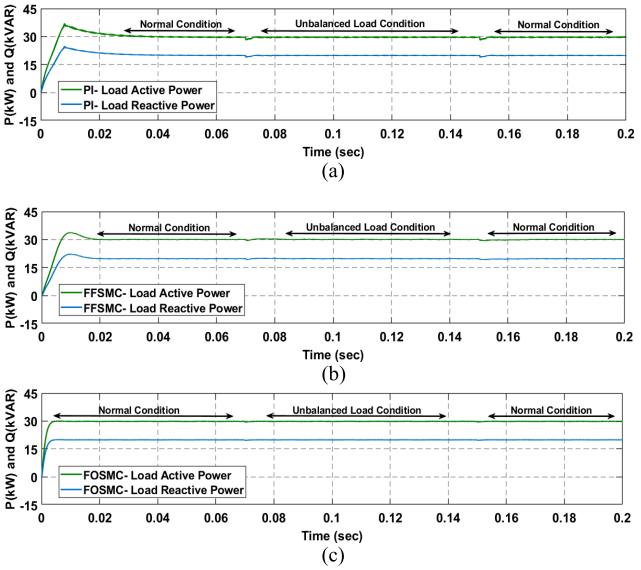

FIGURE 14. (a) Load Active and Reactive power under unbalanced load conditions with D-STATCOM while employing PI control (b) Load Active and Reactive power under unbalanced load conditions with D-STATCOM while employing FFSMC (c) Load Active and Reactive power under unbalanced load conditions with D-STATCOM while employing FOSMC.

Fig. 15(a) shows the reactive power injected by D-STATCOM under unbalanced load conditions while employing PI control. Fig. 15(b) shows the reactive power injected by D-STATCOM under unbalanced load conditions while employing FFSMC. Fig. 16 shows the variation of α, k_d and k_q, and its influence on rise time, convergence time, tracking error, and time to reach the steady-state under unbalanced load conditions. The optimum value of α can be retrieved by varying it from 0 to 0.9. Initially, the value of the fractional coefficient α is chosen from [65]. From Fig. 16(a), it can be observed that the increase of $\alpha = 0.8$ increases the tracking error and chattering. Likewise, the decrease of $\alpha = 0.2$ increases the overshoot, rise time, and time to reach the steady-state, can be seen in Fig. 16(c). In the context of k_d and k_q, the initial values are selected from [69]. The decrease in the values of k_d and k_q results in the increase

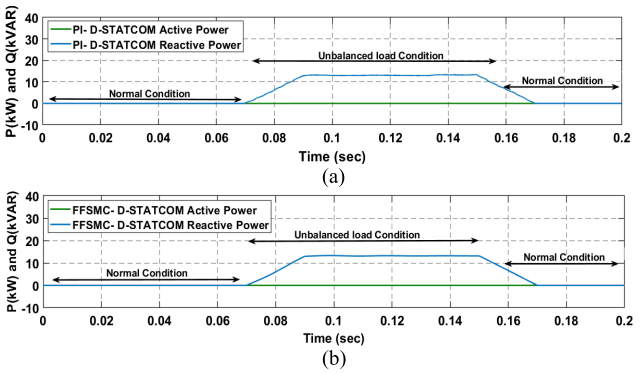

FIGURE 15. (a) Injected Reactive power by D-STATCOM under voltage sag/swell while employing PI control (b) Injected Reactive power by D-STATCOM under voltage sag/swell while employing FFSMC.

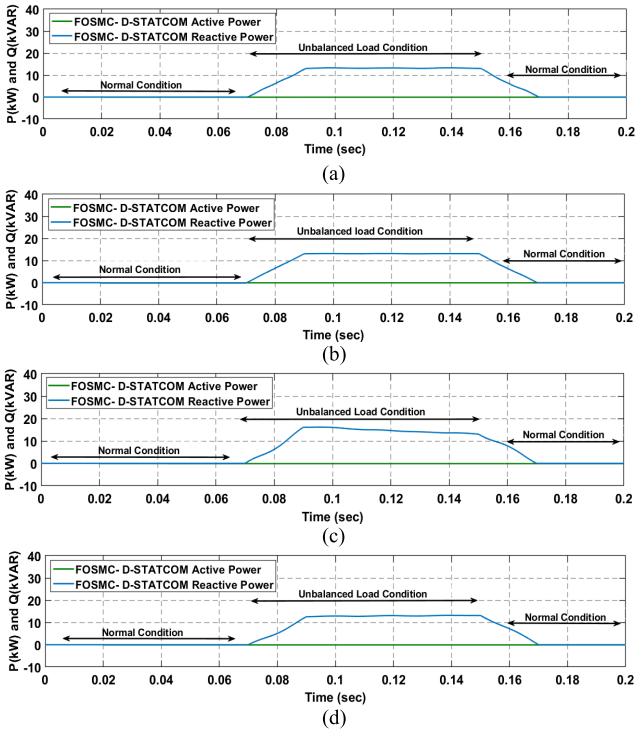

FIGURE 16. (a) Injected reactive power by D-STATCOM under unbalanced load conditions while employing FOSMC with $\alpha = 0.2$ and k_d, $k_q = 5 \times 10^6$ (b) Injected reactive power by D-STATCOM under Unbalanced load conditions while employing FOSMC $\alpha = 0.5$ and k_d, $k_q = 5 \times 10^6$ (c) Injected reactive power by D-STATCOM under unbalanced load conditions while employing FOSMC $\alpha = 0.8$ and k_d, $k_q = 5 \times 10^6$ (d) Injected reactive power by D-STATCOM under unbalanced load conditions while employing FOSMC $\alpha = 0.5$ and k_d, $k_q = 3 \times 10^4$.

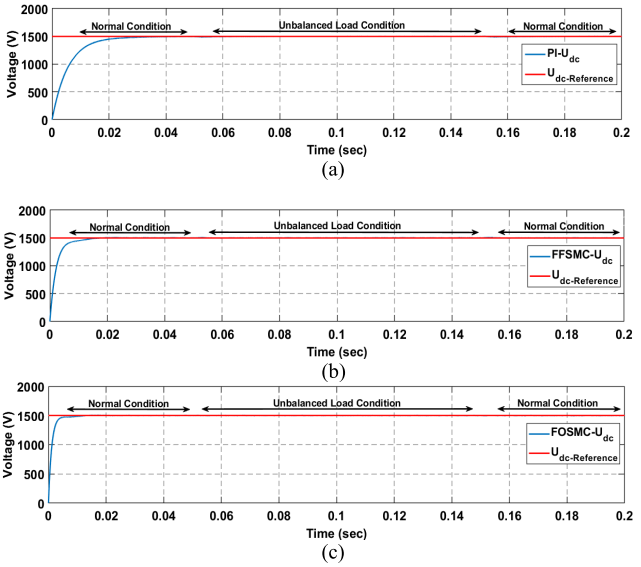

FIGURE 17. (a) dc voltage of D-STATCOM under unbalanced load conditions while employing PI Control (b) dc voltage of D-STATCOM under unbalanced load conditions while employing FFSMC (c) dc voltage of D-STATCOM under unbalanced load conditions while employing FOSMC.

of tracking error and the time to reach the steady-state and it can be seen in Fig. 16(d). Meanwhile, the increase of k_d and k_q results in the decrease of tracking error and the time to reach the steady-state. Therefore, the value of FOSMC parameters must be selected in such a way that a compromise is achieved among the rise time, overshoot, convergence time, tracking error, overall damping along with chattering free smooth output. Therefore, the reference reactive power value is admirable tracked by the controlled trajectories when α is selected to be 0.5 and k_d, k_q are selected to be 5×10^6, evidenced in Fig. 16(b). The peak overshoot and convergence time are enhanced because of non-integer order instantaneous error as per the major characteristic of FOSMC. It can be noted that the proposed FOSMC illustrates the exceptional execution over the FFSMC and PI control in the reactive power tracking, due to the fact that the proposed FOSMC is competent of precisely tracking the reference value with the lowest chattering.

Fig. 17(a) shows the dc voltage of D-STATCOM under unbalanced load conditions while employing PI control. Fig. 17(b) shows the dc voltage of D-STATCOM under unbalanced load conditions while employing FFSMC. Fig. 17(c) shows the dc voltage of D-STATCOM under unbalanced load conditions while employing the proposed FOSMC. It can be noted that the execution of the proposed FOSMC is exceptional to FFSMC and PI control regarding fast convergence and fast-tracking.

Table 7 shows the assessment of different control strategies present in the study with the proposed FOSMC. Table 8 shows the assessment of the proposed FOSMC with existing SMC strategies while enhancing power quality. The assessment is made in terms of response time, accuracy, robustness,

TABLE 7. Comparison with different control strategies.

Reference	Control Schemes	Compensation	Controller Complexity
[17]	PI Control	Voltage Sag/Swell	Low
[36]	Hysteresis Control	Unbalanced Load	Medium
[38]	FLC	Voltage Sag/Swell	Low
[71]	MPC	Voltage Unbalanced	Medium
Proposed	FOSMC	Voltage Sag/Swell and Unbalanced Load	Lowest

TABLE 8. X-tics comparison of proposed FOSMC with current SMC strategies.

X-tics	Proposed FOSMC	[55]	[56]	[80]	[60]
Response Time	Fast	Fast	Fast	Fast	Medium
Accuracy	Very High	High	High	High	High
Robustness	Very High	Medium	High	High	Moderate
Chattering	Lowest	Low	Low	-	Low
Transient Response	Very Fast	Fast	Fast	Fast	Fast
Voltage THD (%)	0.52	-	-	1.02	-
Steady-State Time (s)	0.02	0.3	-	-	-

chattering, THD, and steady-state time. The performance of the proposed control is excellent in all performance parameters.

VI. CONCLUSION

In this paper, the authors have proposed a FOSMC based D-STATCOM to compensate the low power distribution system under disturbances such as voltage sag/swell and unbalanced load conditions. Besides, the performance of the FOSMC under its parametric variations is discussed as well. The complete system is demonstrated with a model of 400V, 180kVA radial distributor along with D-STATCOM under two test scenarios in MATLAB/Simulink environment. In the first test scenario, the grid transients (voltage sag/swell) are considered at the LV AC bus. Likewise, in the second test scenario, the unbalanced load conditions are considered at the LV AC bus. D-STATCOM sustains the voltage at LV AC bus by injecting/absorbing a certain extent of reactive power under voltage sag/swell and unbalanced load conditions.

The results of the proposed controller are compared with fixed frequency sliding mode control (FFSMC) and conventional proportional-integral (PI) control. The results validate the superiority of the proposed controller in terms of rapid tracking, fast convergence, and overall damping with very low THD, and VUF. In the first test scenario, the voltage THD of proposed FOSMC during voltage sag/swell results in 0.52% in contrast to FFSMC and PI control which have THD of 0.84% and 2.17% respectively. In the second test scenario, the voltage THD of proposed FOSMC during unbalanced load conditions results in 0.97% in contrast to FFSMC and PI control which have THD of 1.96% and 3.63%. Likewise, the VUF under unbalanced load conditions with proposed FOSMC is 0.0014% in contrast to FFSMC and PI control which have VUF of 0.02% and 0.71%.

In terms of assessment with existing SMC schemes, the proposed FOSMC has a very high response time, very high accuracy, very high robustness, lowest chattering along with low THD and VUF. The proposed model could be realized on the hardware platform for real-time verification purposes in future applications.

ACKNOWLEDGMENT

The authors would like to acknowledge the support of Prince Sultan University for paying the Article Processing Charges (APC) of this publication and for having rendered their technical support. The authors also thank the Clean and Resilient Energy Systems (CARES) Laboratory, Texas A&M University, Galveston, USA, and Bahria University, Islamabad, Pakistan, for the technical expertise provided.

REFERENCES

[1] A. Q. Al-Shetwi, M. A. Hannan, K. P. Jern, A. A. Alkahtani, and A. E. P. Abas, "Power quality assessment of grid-connected PV system in compliance with the recent integration requirements," *Electronics*, vol. 9, no. 2, p. 366, Feb. 2020.

[2] A. D. J. C. Leal, C. L. T. Rodríguez, and F. Santamaria, "Comparative of power calculation methods for single-phase systems under sinusoidal and non-sinusoidal operation," *Energies*, vol. 13, no. 17, p. 4322, Aug. 2020.

[3] E. Hossain, M. R. Tür, S. Padmanaban, S. Ay, and I. Khan, "Analysis and mitigation of power quality issues in distributed generation systems using custom power devices," *IEEE Access*, vol. 6, pp. 16816–16833, 2018.

[4] F. R. Islam, K. Prakash, K. A. Mamun, A. Lallu, and H. R. Pota, "Aromatic network: A novel structure for power distribution system," *IEEE Access*, vol. 5, pp. 25236–25257, 2017.

[5] A. A. Alkahtani, S. T. Y. Alfalahi, A. A. Athamneh, A. Q. Al-Shetwi, M. B. Mansor, M. A. Hannan, and V. G. Agelidis, "Power quality in microgrids including supraharmonics: Issues, standards, and mitigations," *IEEE Access*, vol. 8, pp. 127104–127122, 2020.

[6] B. Liu, K. Meng, Z. Y. Dong, P. K. C. Wong, and T. Ting, "Unbalance mitigation via phase-switching device and static var compensator in low-voltage distribution network," *IEEE Trans. Power Syst.*, vol. 35, no. 6, pp. 4856–4869, Nov. 2020.

[7] E. A. Belati, C. F. Nascimento, H. de Faria, E. H. Watanabe, and A. Padilha-Feltrin, "Allocation of static var compensator in electric power systems considering different load levels," *J. Control, Autom. Electr. Syst.*, vol. 30, no. 1, pp. 1–8, Feb. 2019.

[8] J. Pereda and T. C. Green, "Direct modular multilevel converter with six branches for flexible distribution networks," *IEEE Trans. Power Del.*, vol. 31, no. 4, pp. 1728–1737, Aug. 2016.

[9] *IEEE Guide for Specification of Transmission Static Synchronous Compensator (STATCOM) Systems*, IEEE Standard 1052-2018, Apr. 2019, pp. 1–115.

[10] T. M. T. Thentral, R. Jegatheesan, and K. Vijayakumar, "Unified power quality conditioner with reduced switch topology for distributed networks," *Wireless Netw.*, vol. 27, no. 2, pp. 909–923, Feb. 2021.

[11] M. Bagheri, V. Nurmanova, O. Abedinia, and M. S. Naderi, "Enhancing power quality in microgrids with a new online control strategy for DSTATCOM using reinforcement learning algorithm," *IEEE Access*, vol. 6, pp. 38986–38996, 2018.

[12] M. N. I. Sarkar, L. G. Meegahapola, and M. Datta, "Reactive power management in renewable rich power grids: A review of grid-codes, renewable generators, support devices, control strategies and optimization algorithms," *IEEE Access*, vol. 6, pp. 41458–41489, 2018.

[13] S. Jadhav and N. Jangle, "Improvement in power quality performance using S-transform based D-STATCOM," in *Proc. IEEE Int. Conf. Syst., Comput., Automat. Netw. (ICSCA)*, Jul. 2018, pp. 1–6.

[14] K. Sayahi, A. Kadri, F. Bacha, and H. Marzougui, "Implementation of a D-STATCOM control strategy based on direct power control method for grid connected wind turbine," *Int. J. Electr. Power Energy Syst.*, vol. 121, Oct. 2020, Art. no. 106105.

[15] A. Khoshooei, J. S. Moghani, I. Candela, and P. Rodriguez, "Control of D-STATCOM during unbalanced grid faults based on DC voltage oscillations and peak current limitations," *IEEE Trans. Ind. Appl.*, vol. 54, no. 2, pp. 1680–1690, Mar. 2018.

[16] W.-N. Chang and C.-H. Liao, "Development of an SDBC-MMCC-based DSTATCOM for real-time single-phase load compensation in three-phase power distribution systems," *Energies*, vol. 12, no. 24, p. 4705, Dec. 2019.

[17] R. Pandey, R. Tripathi, and T. Hanamoto, "Comprehensive analysis of LCL filter interfaced cascaded H-bridge multilevel inverter-based DSTATCOM," *Energies*, vol. 10, no. 3, p. 346, Mar. 2017.

[18] S. M. Fazeli, H. W. Ping, N. B. A. Rahim, and B. T. Ooi, "Individual-phase control of 3-phase 4-wire voltage–source converter," *IET Power Electron.*, vol. 7, no. 9, pp. 2354–2364, Sep. 2014.

[19] L. Wang, W.-S. Liu, C.-C. Yeh, C.-H. Yu, X.-Y. Lu, B.-L. Kuan, H.-Y. Wu, and A. V. Prokhorov, "Reduction of three-phase voltage unbalance subject to special winding connections of two single-phase distribution transformers of a microgrid system using a designed D-STATCOM controller," *IEEE Trans. Ind. Appl.*, vol. 54, no. 3, pp. 2002–2011, May/Jun. 2018.

[20] F. Hamoud, M. L. Doumbia, and A. Cheriti, "Voltage sag and swell mitigation using D-STATCOM in renewable energy based distributed generation systems," in *Proc. 12th Int. Conf. Ecol. Vehicles Renew. Energies (EVER)*, Monte Carlo, Monaco, Apr. 2017, pp. 1–6.

[21] P. E. Melin, J. I. Guzman, F. A. Hernandez, C. R. Baier, J. A. Muñoz, J. R. Espinoza, and E. E. Espinosa, "Analysis and control strategy for a current-source based D-STATCOM towards minimum losses," *Int. J. Electr. Power Energy Syst.*, vol. 116, Mar. 2020, Art. no. 105532, doi: 10.1016/j.ijepes.2019.105532.

[22] Y. A. Kadi and F. Z. Baghli, "PV-STATCOM in photovoltaic systems under variable solar radiation and variable unbalanced nonlinear loads," *Int. J. Electr. Electron. Eng. Telecommun.*, vol. 10, no. 1, pp. 36–48, Jan. 2021.
[23] A. H. Elmetwaly, A. A. Eldesouky, and A. A. Sallam, "An adaptive D-FACTS for power quality enhancement in an isolated microgrid," *IEEE Access*, vol. 8, pp. 57923–57942, 2020, doi: 10.1109/ACCESS.2020.2981444.
[24] M. Deben Singh, R. K. Mehta, and A. K. Singh, "Integrated fuzzy-PI controlled current source converter based D-STATCOM," *Cogent Eng.*, vol. 3, no. 1, Dec. 2016, Art. no. 1138921.
[25] H. A. Soodi and A. M. Vural, "Design, optimization and experimental verification of a low cost two-microcontroller based single-phase STATCOM," *IETE J. Res.*, pp. 1–11, Jan. 2021, doi: 10.1080/03772063.2021.1875270.
[26] Sujono, I. Sudiharto, and O. A. Qudsi, "Application of D-STATCOM to reduce unbalanced load using synchronous reference frame theory," in *Proc. 10th Electr. Power, Electron., Commun., Controls Informat. Seminar (EECCIS)*, Malang, Indonesia, Aug. 2020, pp. 65–70, doi: 10.1109/EECCIS49483.2020.9263476.
[27] R. M. Abdalaal and C. N. M. Ho, "A supervisory remote management system for parallel operation of modularized D-STATCOM," in *Proc. IEEE Appl. Power Electron. Conf. Expo. (APEC)*, New Orleans, LA, USA, Mar. 2020, pp. 989–994, doi: 10.1109/APEC39645.2020.9124219.
[28] J. M. L. da Fonseca, F. K. de Araújo Lima, F. L. Tofoli, and C. G. C. Branco, "Three-phase phase-locked loop algorithm and application to a static synchronous compensator," *Electr. Power Syst. Res.*, vol. 192, Mar. 2021, Art. no. 106924, doi: 10.1016/j.epsr.2020.106924.
[29] R. Geethamani, N. Jayalakshmi, M. R. Meera, M. S. S. Sundari, M. Upadhyaya, G. K. J. Samuel, and J. J. Poornima, "Realization of cascaded hybrid bridge multilevel inverter using distribution static compensator," *Mater. Today, Proc.*, Jan. 2021, doi: 10.1016/j.matpr.2020.10.871.
[30] K. Wang, S. Gao, Z. Shi, L. Liu, A. Ren, Y. Wang, L. Tian, and J. Gao, "Research on reactive power coordinated control strategy of doubly-fed wind farm considering STATCOM," in *Proc. IEEE 4th Conf. Energy Internet Energy Syst. Integr. (EI2)*, Wuhan, China, Oct. 2020, pp. 1275–1279, doi: 10.1109/EI250167.2020.9346760.
[31] B. Jahnavi, S. B. Karanki, and P. K. Kar, "Power quality improvement with D-STATCOM using combined PR and comb filter-controller," in *Proc. 1st Int. Conf. Power Electron. Energy (ICPEE)*, Bhubaneswar, India, Jan. 2021, pp. 1–6, doi: 10.1109/ICPEE50452.2021.9358692.
[32] Q. Huang, X. Zou, D. Zhu, and Y. Kang, "Scaled current tracking control for doubly fed induction generator to ride-through serious grid faults," *IEEE Trans. Power Electron.*, vol. 31, no. 3, pp. 2150–2165, Mar. 2016.
[33] M. S. Zaky, "A self-tuning PI controller for the speed control of electrical motor drives," *Electr. Power Syst. Res.*, vol. 119, pp. 293–303, Feb. 2015.
[34] H. Chen, B. Sun, J. Qu, and K. Fu, "An improved deadbeat control strategy for D-STATCOM based on frequency-adaptive repetitive predictor," in *Proc. IEEE Int. Conf. Cyber Technol. Automat., Control, Intell. Syst. (CYBER)*, Shenyang, China, Jun. 2015, pp. 1720–1725.
[35] J. Kim, J. Hong, and H. Kim, "Improved direct deadbeat voltage control with an actively damped inductor-capacitor plant model in an islanded AC microgrid," *Energies*, vol. 9, no. 11, p. 978, Nov. 2016.
[36] M. Kullan, R. Muthu, J. B. Mervin, and V. Subramanian, "Design of DSTATCOM controller for compensating unbalances," *Circuits Syst.*, vol. 7, no. 9, pp. 2362–2372, 2016.
[37] S. Tahir, J. Wang, M. Baloch, and G. Kaloi, "Digital control techniques based on voltage source inverters in renewable energy applications: A review," *Electronics*, vol. 7, no. 2, p. 18, Feb. 2018.
[38] D. Amoozegar, "DSTATCOM modelling for voltage stability with fuzzy logic PI current controller," *Int. J. Elect. Power Energy Syst.*, vol. 76, pp. 129–135, Mar. 2016.
[39] Y. Jiang, C. Yang, and M. Hongbin, "A review of fuzzy logic and neural network based intelligent control design for discrete-time system," *Discrete Dyn. Nature Soc.*, vol. 2016, pp. 11–17, Jan. 2016.
[40] R. Çöteli, H. Açikgöz, B. Dandil, and S. Tuncer, "Real-time implementation of three-level inverter-based D-STATCOM using neuro-fuzzy controller," *TURKISH J. Electr. Eng. Comput. Sci.*, vol. 26, no. 4, pp. 2088–2103, Jul. 2018.
[41] K.-H. Tan, F.-J. Lin, C.-Y. Tsai, and Y.-R. Chang, "A distribution static compensator using a CFNN-AMF controller for power quality improvement and DC-link voltage regulation," *Energies*, vol. 11, no. 8, p. 1996, Aug. 2018.
[42] M. Badoni, A. Singh, B. Singh, and H. Saxena, "Real-time implementation of active shunt compensator with adaptive SRLMMN control technique for power quality improvement in the distribution system," *IET Gener., Transmiss. Distrib.*, vol. 14, no. 8, pp. 1598–1606, Apr. 2020.
[43] J. I. Y. Ota, Y. Shibano, and H. Akagi, "A phase-shifted PWM D-STATCOM using a modular multilevel cascade converter (SSBC)—Part II: Zero-voltage-ride-through capability," *IEEE Trans. Ind. Appl.*, vol. 51, no. 1, pp. 289–296, Jan. 2015.
[44] H. Sufiev, Y. Haddad, L. Barenboim, and J. Soler, "Dynamic SDN controller load balancing," *Future Internet*, vol. 11, no. 3, p. 75, Mar. 2019.
[45] Y. Ma, X. Sun, and X. Zhou, "Research on D-STATCOM double closed-loop control method based on improved first-order linear active disturbance rejection technology," *Energies*, vol. 13, no. 15, p. 3958, Aug. 2020, doi: 10.3390/en13153958.
[46] W. Rohouma, R. S. Balog, A. A. Peerzada, and M. M. Begovic, "D-STATCOM for harmonic mitigation in low voltage distribution network with high penetration of nonlinear loads," *Renew. Energy*, vol. 145, pp. 1449–1464, Jan. 2020, doi: 10.1016/j.renene.2019.05.134.
[47] J. Hu, J. Zhu, G. Lei, G. Platt, and D. G. Dorrell, "Multi-objective model-predictive control for high-power converters," *IEEE Trans. Energy Convers.*, vol. 28, no. 3, pp. 652–663, Sep. 2013, doi: 10.1109/TEC.2013.2270557.
[48] W. Rohouma, M. Metry, R. S. Balog, A. A. Peerzada, and M. M. Begovic, "Adaptive model predictive controller to reduce switching losses for a capacitor-less D-STATCOM," *IEEE Open J. Power Electron.*, vol. 1, pp. 300–311, 2020, doi: 10.1109/OJPEL.2020.3015352.
[49] D. Sotelo, A. Favela-Contreras, V. V. Kalashnikov, and C. Sotelo, "Model predictive control with a relaxed cost function for constrained linear systems," *Math. Problems Eng.*, vol. 2020, pp. 1–10, Mar. 2020, doi: 10.1155/2020/7485865.
[50] T. D. C. Busarello, K. Zeb, M. A. Sarwar, and H. J. Kim, "Three-phase D-STATCOM with digital current control strategy in abc-reference frame," in *Proc. 3rd Int. Conf. Comput., Math. Eng. Technol. (iCoMET)*, Sukkur, Pakistan, Jan. 2020, pp. 1–6, doi: 10.1109/iCoMET48670.2020.9073883.
[51] H. P. Vemuganti, D. Sreenivasarao, and G. S. Kumar, "A three-phase transformer based T-type topology for DSTATCOM application," *Int. J. Electron.*, pp. 1–21, Feb. 2021, doi: 10.1080/00207217.2020.1870733.
[52] O. D. Montoya, W. Gil-González, and J. C. Hernández, "Efficient operative cost reduction in distribution grids considering the optimal placement and sizing of D-STATCOMs using a discrete-continuous VSA," *Appl. Sci.*, vol. 11, no. 5, p. 2175, Mar. 2021, doi: 10.3390/app11052175.
[53] B. Mahdad, "A novel tree seed algorithm for optimal reactive power planning and reconfiguration based STATCOM devices and PV sources," *Social Netw. Appl. Sci.*, vol. 3, Feb. 2021, Art. no. 336, doi: 10.1007/s42452-021-04338-5.
[54] X. Su, M. Han, J. Guerrero, and H. Sun, "Microgrid stability controller based on adaptive robust total SMC," *Energies*, vol. 8, no. 3, pp. 1784–1801, Mar. 2015.
[55] G. Shahgholian and Z. Azimi, "Analysis and design of a DSTATCOM based on sliding mode control strategy for improvement of voltage sag in distribution systems," *Electronics*, vol. 5, no. 4, p. 41, Jul. 2016.
[56] S. Bouafia, A. Benaissa, S. Barkat, and M. Bouzidi, "Second order sliding mode control of three-level four-leg DSTATCOM based on instantaneous symmetrical components theory," *Energy Syst.*, vol. 9, no. 1, pp. 79–111, Feb. 2018.
[57] K. D. E. Kerrouche, L. Wang, A. Mezouar, L. Boumediene, and A. Van Den Bossche, "Fractional-order sliding mode control for D-STATCOM connected wind farm based DFIG under voltage unbalanced," *Arabian J. Sci. Eng.*, vol. 44, no. 3, pp. 2265–2280, Mar. 2019.
[58] S. Mishra and P. K. Ray, "Nonlinear modeling and control of a photovoltaic fed improved hybrid DSTATCOM for power quality improvement," *Int. J. Electr. Power Energy Syst.*, vol. 75, pp. 245–254, Feb. 2016.
[59] M. Xia and Y. Mao, "Integral sliding mode control strategy of D-STATCOM for unbalanced load compensation under various disturbances," *Math. Problems Eng.*, vol. 2013, pp. 1–14, Jan. 2013.
[60] J. Wu, Q. Chen, M. Du, and S. Yu, "Sliding-mode variable structure controller for cascade STATic var COMpensator," *IET Power Electron.*, vol. 6, no. 2, pp. 343–352, Feb. 2013.
[61] H. Gong, Y. Wang, Y. Li, X. Li, and L. Wei, "An input-output feedback linearized sliding mode control for D-STATCOM," *Automat. Electr. Power Syst.*, vol. 40, no. 5, pp. 102–108, 2016.

[62] E. Hashemzadeh, M. Khederzadeh, M. R. Aghamohammadi, and M. Asadi, "A robust control for D-STATCOM under variations of DC-link capacitance," *IEEE Trans. Power Electron.*, vol. 36, no. 7, pp. 8325–8333, Jul. 2021, doi: 10.1109/TPEL.2020.3026092.
[63] R. Gupta and A. Ghosh, "Frequency-domain characterization of sliding mode control of an inverter used in DSTATCOM application," *IEEE Trans. Circuits Syst. I, Reg. Papers*, vol. 53, no. 3, pp. 662–676, Mar. 2006.
[64] K. D. E. Kerrouche, E. Lodhi, M. B. Kerrouche, L. Wang, F. Zhu, and G. Xiong, "Modeling and design of the improved D-STATCOM control for power distribution grid," *Social Netw. Appl. Sci.*, vol. 2, no. 9, Sep. 2020, Art. no. 1519, doi: 10.1007/s42452-020-03315-8.
[65] M. B. Delghavi, S. Shoja-Majidabad, and A. Yazdani, "Fractional-order sliding-mode control of islanded distributed energy resource systems," *IEEE Trans. Sustain. Energy*, vol. 7, no. 4, pp. 1482–1491, Oct. 2016.
[66] S. J. Gambhire, D. R. Kishore, P. S. Londhe, and S. N. Pawar, "Review of sliding mode based control techniques for control system applications," *Int. J. Dyn. Control*, vol. 9, no. 1, pp. 363–378, Mar. 2021, doi: 10.1007/s40435-020-00638-7.
[67] Q. Zhou, M. Shahidehpour, A. Paaso, S. Bahramirad, A. Alabdulwahab, and A. Abusorrah, "Distributed control and communication strategies in networked microgrids," *IEEE Commun. Surveys Tuts.*, vol. 22, no. 4, pp. 2586–2633, 4th Quart., 2020.
[68] P. Li, J. Wang, L. Xiong, S. Huang, Z. Wang, and M. Ma, "SSCI mitigation of grid-connected DFIG wind turbines with fractional-order sliding mode controller," *Wind Energy*, vol. 23, no. 7, pp. 1564–1577, 2020.
[69] T. Ahmed, A. Waqar, E. A. Al-Ammar, W. Ko, Y. Kim, M. Aamir, and H. U. R. Habib, "Energy management of a battery storage and D-STATCOM integrated power system using fractional order sliding mode control," *CSEE J. Power Energy Syst.*, early access, Oct. 6, 2020, doi: 10.17775/CSEEJPES.2020.02530.
[70] M. A. Hannan, "Effect of DC capacitor size on D-STATCOM voltage regulation performance evaluation," *Press Electr. Rev.*, vol. 88, pp. 243–246, Jan. 2012.
[71] A. S. Emam, A. M. Azmy, and E. M. Rashad, "Enhanced model predictive control-based STATCOM implementation for mitigation of unbalance in line voltages," *IEEE Access*, vol. 8, pp. 225995–226007, 2020.
[72] M. B. Delghavi and A. Yazdani, "Sliding-mode control of AC voltages and currents of dispatchable distributed energy resources in master-slave-organized inverter-based microgrids," *IEEE Trans. Smart Grid*, vol. 10, no. 1, pp. 980–991, Jan. 2019.
[73] V. Kumar and I. Ali, "Fractional order sliding mode approach for chattering free direct power control of DC/AC converter," *IET Power Electron.*, vol. 12, no. 13, pp. 3600–3610, Nov. 2019.
[74] T. Ahmed, A. Waqar, T. Hussain, E. A. Al-Ammar, M. Zahid, and H. U. R. Habib, "Fractional order sliding mode control for voltage source voltage converters under reconfiguration," in *Proc. Int. Symp. Recent Adv. Electr. Eng. Comput. Sci. (RAEE CS)*, Islamabad, Pakistan, Oct. 2020, pp. 1–6.
[75] F. Sebaaly, H. Vahedi, H. Y. Kanaan, N. Moubayed, and K. Al-Haddad, "Sliding mode fixed frequency current controller design for grid-connected NPC inverter," *IEEE J. Emerg. Sel. Topics Power Electron.*, vol. 4, no. 4, pp. 1397–1405, Dec. 2016.
[76] S. Pati, K. B. Mohanty, S. K. Kar, and D. Panda, "Voltage and frequency stabilization of a micro hydro-PV based hybrid micro grid using STATCOM equipped with battery energy storage system," in *Proc. IEEE Int. Conf. Power Electron., Drives Energy Syst. (PEDES)*, Trivandrum, India, Dec. 2016, pp. 1–5.
[77] L. Xiong, J. Wang, X. Mi, and M. W. Khan, "Fractional order sliding mode based direct power control of grid-connected DFIG," *IEEE Trans. Power Syst.*, vol. 33, no. 3, pp. 3087–3096, May 2018.
[78] A. Susperregui, J. M. Herrero, M. I. Martinez, G. Tapia-Otaegui, and X. Blasco, "Multi-objective optimisation-based tuning of two second-order sliding-mode controller variants for DFIGs connected to non-ideal grid voltage," *Energies*, vol. 12, no. 19, p. 3782, Oct. 2019.
[79] C. Yeroğlu and G. Kavuran, "Sliding mode controller design with fractional order differentiation: Applications for unstable time delay systems," *TURKISH J. Electr. Eng. Comput. Sci.*, vol. 22, no. 5, pp. 1270–1286, 2014.
[80] V. Rajakumar, K. Anbukumar, and I. Selwynraj, "Sliding mode controller-based voltage source inverter for power quality improvement in microgrid," *IET Renew. Power Gener.*, vol. 14, no. 11, pp. 1860–1872, Aug. 2020.
[81] J. Wang, M. C. Lee, J. H. Kim, and H. H. Kim, "Fast fractional-order terminal sliding mode control for seven-axis robot manipulator," *Appl. Sci.*, vol. 10, no. 21, 2020, Art. no. 7757, doi: 10.3390/app10217757.
[82] Y. Li, J. Zhang, and Q. Wu, *Adaptive Sliding Mode Neural Network Control for Nonlinear Systems: Emerging Methodologies and Applications in Modelling*. New York, NY, USA: Academic, 2020, pp. 1–16, doi: 10.1016/B978-0-12-815372-7.00001-X.
[83] H. H. Alhelou, M. Hamedani-Golshan, T. Njenda, and P. Siano, "A survey on power system blackout and cascading events: Research motivations and challenges," *Energies*, vol. 12, no. 4, p. 682, Feb. 2019.
[84] O. Eray and S. Tokat, "The design of a fractional-order sliding mode controller with a time-varying sliding surface," *Trans. Inst. Meas. Control*, vol. 42, no. 5, pp. 3196–3215, 2020.
[85] R. Matušu, B. Şenol, and L. Pekař, "Robust stability of fractional-order linear time-invariant systems: Parametric versus unstructured uncertainty models," *Complexity*, vol. 2018, Aug. 2018, Art. no. 8073481.
[86] P. Li, L. Xiong, Z. Wang, M. Ma, and J. Wang, "Fractional-order sliding mode control for damping of subsynchronous control interaction in DFIG-based wind farms," *Wind Energy*, vol. 23, no. 3, pp. 749–762, Mar. 2020.
[87] P. E. Melin, J. I. Guzman, F. A. Hernandez, C. R. Baier, J. A. Muñoz, J. R. Espinoza, and E. E. Espinosa, "Analysis and control strategy for a current-source based D-STATCOM towards minimum losses," *Int. J. Electr. Power Energy Syst.*, vol. 116, Mar. 2020, Art. no. 105532, doi: 10.1016/j.ijepes.2019.105532.
[88] I. Mehouachi, M. Abbes, and S. Chebbi, "Design of a high power D-STATCOM based on the isolated dual-converter topology," *Int. J. Electr. Power Energy Syst.*, vol. 106, pp. 401–410, Mar. 2019, doi: 10.1016/j.ijepes.2018.10.025.

TOQEER AHMED received the B.E. degree in electrical engineering from Hamdard University, Islamabad, Pakistan, and the M.S. degree in electrical engineering from Bahria University, Islamabad. He is currently an Electrical Engineer by Profession. He is also working as a Faculty Member with the Department of Center for Advanced Electronics and Photovoltaic Engineering (CAEPE), International Islamic University, Islamabad. He is a part of multiple international joint research projects. He has also experience in teaching laboratory courses to undergraduate students. His research interests include artificial intelligence, machine learning, deep learning, microgrid operation and control, modeling and simulation, energy management systems, advanced electronics, power electronics, power systems reliability and stability, power quality, FACTs devices, non-linear control techniques, and its application in the power industry. He is a member of the Pakistan Engineering Council (PEC) and the Institution of Engineers, Pakistan (IEP). He was a Gold Medalist in his bachelor's degree.

ASAD WAQAR received the degree in electrical engineering from UET Taxila, in 2002, the master's degree in electrical power engineering from RWTH Aachen Germany, in 2011, and the Ph.D. degree in electrical engineering from the Huazhong University of Science and Technology, China, in 2016. He worked for different industries for several years. He is currently working as an Associate Professor with the Department of Electrical Engineering, Bahria University, Islamabad, Pakistan. He has successfully supervised more than 30 master's thesis students. He is supervising three Ph.D. students at Bahria University as well. He has published research articles in many reputed international journals. His research interests include smart grids, microgrid operation and control, power quality, power electronics, network reinforcement planning, demand side management, and big data analysis in power systems. He serves as an Active Reviewer for *Applied Energy*, *International Transactions on Electrical Energy Systems*, IEEE Access, *Renewable and Sustainable Energy Reviews*, and *International Journal for Engineering Science and Technology*.

RAJVIKRAM MADURAI ELAVARASAN received the B.E. degree in electrical and electronics engineering from Anna University, Chennai, India, and the M.E. degree in power system engineering from the Thiagarajar College of Engineering, Madurai. He held an Associate Technical Operations with the IBM Global Technology Services Division. He was as an Assistant Professor with the Department of Electrical and Electronics, Sri Venkateswara College of Engineering, Sriperumbudur, India. He is currently a Visiting Scholar with the Clean and Resilient Energy Systems Laboratory, Texas A&M University, Galveston, TX, USA. His research interests include renewable energy and smart grids, wind energy research, power system operation and control, and artificial intelligence control techniques. He was a Gold Medalist in his master's degree. He serves as a Recognized Reviewer for reputed journals, such as the IEEE Systems Journal, IEEE Access, the *IEEE Communications Magazine*, the *International Transactions on Electrical Energy Systems* (Wiley), *Energy Sources, Part A: Recovery, Utilization and Environmental Effects* (Taylor and Francis), *Scientific Reports* (Springer Nature), *Chemical Engineering Journal* (Elsevier), *CFD Letters*, and *3 Biotech* (Springer).

JUNAID IMTIAZ received the Bachelor of Electrical Engineering degree, in 2007, the master's degree from the University of Leicester, U.K., in 2010, and the Ph.D. degree in electronics and communication engineering from Hanyang University, South Korea, in 2016. He worked with different engineering firms. He is currently the Head of the Department of Electrical Engineering, Bahria University, Islamabad, Pakistan. He has vast research and academics experience. His research interests include power efficiency for communication engineering applications, power analysis for future communication systems, and security aspect of communication networks.

MANOHARAN PREMKUMAR (Member, IEEE) was born in Coimbatore, India. He received the B.E. degree in electrical and electronics engineering from the Sri Ramakrishna Institute of Technology, Coimbatore, in 2004, the M.E. degree in applied electronics from the Anna University of Technology, Coimbatore, in 2010, and the Ph.D. degree from Anna University, Chennai, India, in 2019. He is currently working as an Associate Professor of electrical and electronics engineering with the Dayananda Sagar College of Engineering, Bengaluru, India. He has more than 12 years of teaching experience, and he has published more than 75 technical articles in various national/international peer-reviewed journals, such as IEEE, Elsevier, and Springer, over 300 citations and an H-index of 11. His current research interests include optimization techniques, including single, multi, and many objectives, solar PV microinverter, solar PV parameter extraction, modern solar PVMPPTs (optimization technique-based), PV array faults, and non-isolated/isolated dc-dc converters for PV systems. He is also serving as an Editor/Reviewer for leading journals, such as IEEE, IET, Wiley, Taylor & Francis, and Springer.

UMASHANKAR SUBRAMANIAM (Senior Member, IEEE) worked as an Associate Professor and the Head with VIT Vellore, and a Senior Research and Development and a Senior Application Engineer in the field of power electronics, renewable energy, and electrical drives. He is currently with the Renewable Energy Laboratory, College of Engineering, Prince Sultan University, Saudi Arabia. He has more than 15 years of teaching, research, and industrial research and development experience. Under his guidance, 24 P.G. students and more than 25 U.G. Students completed the senior design project work. Also, six Ph.D. scholars completed Ph.D. thesis as a Research Associate. He is also involved in collaborative research projects with various international and national level organizations, and research institutions. He has published more than 250 research articles in national and international journals and conferences. He has authored/coauthored/contributed 12 books/chapters and 12 technical articles on power electronics applications in renewable energy and allied areas. He is also a member of IACSIT, IDES, and ISTE. From 2014 to 2016, he was an Executive Member. He received the Danfoss Innovator Award-Mentor, from 2014 to 2015, and from 2017 to 2018, and the Research Award from VIT University, from 2013 to 2018. He received the INAE Summer Research Fellowship for the year 2014. He has taken charge as the Vice-Chair of the IEEE Madras Section and the Chair of IEEE Student Activities, from 2018 to 2019. From 2017 to 2019, he was the Vice-Chair of the IEEE MAS Young Professional by the IEEE Madras Section. He is also an Editor of *Heliyon* (Elsevier).